AD-A056 247 HARVARD UNIV CAMBRIDGE MA DIV OF APPLIED SCIENCES F/G 11/6
STRUCTURAL IMPERFECTIONS IN AMORPHOUS METALS.(U)
MAY 78 F SPAEPEN
UNCLASSIFIED TR-4 N00014-77-C-0002
NL

| OF |
AD
A056247

END
DATE
FILMED
8 -78
DDC

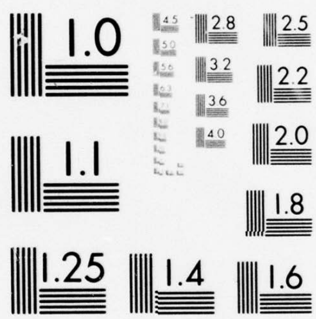

MICROCOPY RESOLUTION TEST CHART
NATIONAL BUREAU OF STANDARDS-1963-A

LEVEL II

Office of Naval Research
Contract N00014-77-C-0002 NR-039-136

STRUCTURAL IMPERFECTIONS IN AMORPHOUS METALS

By
Frans Spaepen

Technical Report No. 4

May 1978

Division of Applied Sciences
Harvard University • Cambridge, Massachusetts

Unclassified 14 TR-4

SECURITY CLASSIFICATION OF THIS PAGE (When Data Entered)

REPORT DOCUMENTATION PAGE		READ INSTRUCTIONS BEFORE COMPLETING FORM
1. REPORT NUMBER Technical Report, No. 4	2. GOVT ACCESSION NO.	3. RECIPIENT'S CATALOG NUMBER
4. TITLE (and Subtitle) STRUCTURAL IMPERFECTIONS IN AMORPHOUS METALS.		5. TYPE OF REPORT & PERIOD COVERED Interim Report
		6. PERFORMING ORG. REPORT NUMBER
7. AUTHOR(s) Frans Spaepen		8. CONTRACT OR GRANT NUMBER(s) N00014-77-C-0002
9. PERFORMING ORGANIZATION NAME AND ADDRESS Division of Applied Sciences Harvard University Cambridge, MA 02138		10. PROGRAM ELEMENT, PROJECT, TASK AREA & WORK UNIT NUMBERS
11. CONTROLLING OFFICE NAME AND ADDRESS		12. REPORT DATE May 1978
		13. NUMBER OF PAGES 33
14. MONITORING AGENCY NAME & ADDRESS (if different from Controlling Office)		15. SECURITY CLASS. (of this report) Unclassified
		15a. DECLASSIFICATION/DOWNGRADING SCHEDULE

16. DISTRIBUTION STATEMENT (of this Report)

This document has been approved for public release and sale; its distribution is unlimited. Reproduction in whole or in part is permitted by the U.S. Government.

17. DISTRIBUTION STATEMENT (of the abstract entered in Block 20, if different from Report)

18. SUPPLEMENTARY NOTES

19. KEY WORDS (Continue on reverse side if necessary and identify by block number)

Amorphous metals
Defects
Vacancy
Dynamic hard sphere model
Atomic transport
Viscosity
Diffusion

20. ABSTRACT (Continue on reverse side if necessary and identify by block number)

The experimental evidence on the existence and nature of imperfections in amorphous metals is reviewed. It derives from observations of microscopic homogeneity, density measurements, positron annihilation studies, inhomogeneous flow and measurements of the various atomic transport coefficients: shear viscosity, diffusivity, structural relaxation rate and crystal growth rate. In contrast with crystal imperfections, which tend to be discrete and localized due to the constraints imposed by the long range periodicity, imperfections in amorphous metals tend to be more extended and over

DD FORM 1473, 1 JAN 73 EDITION OF 1 NOV 65 IS OBSOLETE
S/N 0102-014-6601

Unclassified

SECURITY CLASSIFICATION OF THIS PAGE (When Data Entered)

78 07 12 007

410 457

JDB

Abstract continued

diffuse. This is illustrated by the collapse and annihilation of a vacancy in a two-dimensional amorphous dynamic hard sphere model, and the observations are generalized for other defects in three dimensions. It is concluded that the most fruitful way of describing defects in amorphous metals is as sites with small local perturbations of the "ideal" short range order, which allows local configurational rearrangements. It is suggested that different types of rearrangement (nearest neighbor changes, shear, volume annihilation) are possible at different sites, and that the concentration and lifetime of each type of site determines the time constant of the corresponding atomic transport process.

Office of Naval Research

Contract N00014-77-C-0002 NR-039-136

STRUCTURAL IMPERFECTIONS IN AMORPHOUS METALS

By

Frans Spaepen

Technical Report No. 4

May 1978

The research reported in this document was made possible through support extended the Division of Applied Sciences, Harvard University, by the Office of Naval Research, under Contract N00014-77-C-0002.

Division of Applied Sciences

Harvard University · Cambridge, Massachusetts

I. INTRODUCTION

All amorphous solids, metallic and non-metallic, are actually in states which are configurationally frozen, a particular configuration being specified by the short range order, both topological (TSRO) and compositional (CSRO), and its spatial distribution. Consequently, at any given composition, temperature and pressure a glass may exhibit, depending upon its history, a variety of configurationally frozen states. It will tend to relax toward some state which will be designated, the "fully-relaxed" state. According to the continuous random models for glass structure, this state would be a metastable "ideal glass". If the glass were actually microcrystalline, a possibility now thought to be, in general, unlikely, it would be a single crystal.

Imperfections may be defined as deviations in the structure of the actual glass from that of the fully relaxed glass at $0^{o}K$. In microcrystalline systems the breaking of translational symmetry at points, lines or surfaces would give rise to the same sharp structural discontinuities which are the familiar imperfections of poly-macrocrystals. In contrast, in the absence of the constraints imposed by translational symmetry, imperfections in continuous random structures can be, spatially, very diffuse. Such diffuseness would seem to be a likely feature of metallic structures. In covalently bonded random networks there exist sharper structural discontinuities which can be regarded as dangling bonds, as well as the more diffuse imperfections resulting from abnormal distortions of the interatomic bond angles from their preferred value.

In the first section of this paper we will review and try to interpret some of the evidence, direct and indirect, on the existence and nature of imperfections in metallic glasses. This evidence derives mainly from atomic transport and structural relaxation studies. An important question in the interpretation of these studies is the interrelation and scaling of the time constants for the various processes, in particular: τ_D for diffusive transport, τ_η for viscous flow, τ_V for volume relaxation and τ_c for crystal growth.

In the second section we will illustrate the diffuseness of the defects in amorphous metals by demonstrating the collapse of a localized vacancy created in a two-dimensional dynamic hard sphere system, and speculate about the extension of this basic idea to other defects in three dimensions.

Finally, some general suggestions will be made about the various types of rearrangement that are possible at different defect sites and their implications for the relation between the time constants for atomic transport.

II. SURVEY OF THE EXPERIMENTAL EVIDENCE

1. Microscopic Homogeneity

The first, almost obvious, observation that can be made about amorphous metals is their uniform appearance in the electron or optical microscope. Since the diffraction conditions, which make the direct observation of certain defects such as dislocations possible in crystals, are not present in amorphous materials, the apparent uniformity of the electron images does not provide any conclusions about the absence of defects. The uniform chemical attack of etchants, however, indicates that localized sets of defects (equivalent to crystalline grain boundaries, which are known to be etched under certain conditions) are not present in amorphous metals.

2. Density

The density of amorphous metals is only slightly less ($<1\%$) than that of crystals with a similar composition. This indicates that amorphous metals do not contain any large numbers of vacancy-like defects to the extent that they would result in an appreciable lowering of the density.

Furthermore, it is interesting to note, as Turnbull[1] has pointed out, that the partial atomic volume of the metalloid in transition metal-metalloid alloys (both amorphous and crystalline) is approximately equal to the partial atomic volume of the transition metal. Combined with the short metal-metalloid distance and the high degree of chemical SRO in the first coordination shell as observed in diffraction studies, this indicates that the metal atoms must be packed very closely around the metalloi In other words: there must a correspondingly high degree of topological SRO. The presence of large numbers of localized vacancy-like defects would disrupt this type of SRO and is therefore unlikely. Diffuse defects, i.e., small local perturbations of the SRO are a more likely possibility.

3. Positron Annihilation

This technique is the most direct one available for investigating vacancy-like defects in amorphous materials. In a first type of experiment[2-4], the bulk positron lifetime and the γ-γ angular correlation in amorphous samples are found to be very little different from those in their crystalline counterparts, again indicating the absence of large numbers of localized vacancy-like defects in amorphous systems. The results do not rule out the presence of more diffuse defects. Furthermore, the annihilation spectrum in amorphous systems does not contain a component with a lifetime typical of grain boundary-type defects, which is observed in crystallized samples.[2] This confirms the absence of localized sets of defects and argues against micro-crystalline models for the structure. In a second type of experiment[5] it was observed that the positron lifetime and the γ-γ angular correlation in amorphous metals are not changed much by cold working. This is in contrast with the cold working of crystalline materials, which produces a marked change due to the increased dislocation density. This indicates that the defects introduced during the inhomogeneous deformation of amorphous metals can readily annihilate or become very diffuse, and argues against the presence of localized dislocation-like defects.

4. Inhomogeneous Flow

At high stress levels ($\tau > 10^{-2} \times$ shear modulus) and low temperatures ($T < 0.6\ T_g$) the plastic deformation of amorphous metals becomes localized in narrow planar shear bands, which produces sharp offsets at the specimen surface. The macroscopic analogy between these surface steps and the slip bands formed during plastic deformation of crystals initially led some investigators[6, 7] to invoke the presence of microscopically localized line defects similar to crystalline dislocations to explain the inhomogeneity of the flow. Subsequent investigations, however, have not supported this idea (see previous section on positron annihilation) and since then a number of authors have shown that the localization of flow in amorphous metals can be explained without recourse to localized dislocations: the idea of strain softening due to structural disordering was first introduced by Polk and Turnbull;[8] it was made more explicit by Spaepen,[9] who showed that the local softening in the shear band results from a dynamic equilibrium between the stress-driven creation of defect sites which produce local shear, and their annihilation by diffusion-controlled structural relaxation; recently Argon[10] has shown that, purely on the basis of continuum theory, this mechanism leads to localization of the flow.

5. Atomic Transport

As in crystalline materials, most of the indirect experimental evidence about defects derives from studies of atomic transport. Each of the various transport processes can be characterized by a rate constant (k) or time constant ($\tau = 1/k$): τ_η for viscous flow, τ_D for diffusion, τ_V

for volume (and hence structural) relaxation, τ_c for crystallization. The relative magnitudes and the scaling of these time constants should be related to the concentration and lifetimes of specific defects.

a. Viscous flow

This type of plastic deformation, which occurs at low stress levels ($\tau < 10^{-2}$ x shear modulus), is homogeneous in nature, i.e., each volume element of the specimen contributes to the flow. In the Newtonian viscous regime it can be characterized by the shear viscosity η or a time constant τ_η ($\propto \eta$).

Figure 1 shows some sets of flow data that are typical for the various temperature and stability regimes. Above the melting point, the amorphous phase is stable and its viscosity is low ($\eta \approx 10^{-2}$ poise) (set #1). Around the glass transition temperature T_g, the amorphous phase is still in metastable configurational equilibrium and its viscosity rises steeply with falling temperature due to the rapid increase in SRO which decreases the number of defect sites that can produce local shear (set #2). This development of the SRO also causes a decrease in the number of sites available for configurational rearrangement and hence an increase in the time necessary for structural relaxation. Below T_g, therefore, the amorphous system is kinetically frozen in one particular configuration, and creep experiments performed in this range (sets #4-6) should represent iso-configurational flow. Furthermore, in this regime the system is in unstable equilibrium with respect to the metastable configuration appropriate for the temperature, and any atomic mobility will cause configurational relaxation in that direction (i.e., toward higher time constants). This explains the higher viscosity measured in the repeated set of creep experiments (#6) after they had been annealed for some time during the first set of measurements (#5). It must be emphasized, however, that although creep experiments can in principle be done iso-configurationally (the total strain, which is roughly equal to the fraction of atoms that moved, is only $\sim 10^{-4}$), the occurrence of structural relaxation due to thermal annealing during the experiment has been insufficiently recognized. More reliable experiments, in which proper attention is paid to this problem, are necessary to determine that the measured values of τ_η are associated with well-characterized configurations.

b. Diffusion

The diffusivity around or below T_g is so low ($D < 10^{-16}$ cm^2/sec) that its measurement becomes quite difficult. Only two investigations have been made so far (see Fig. 1): Gupta et al.[16] measured the diffusivity of a Ag^{110} tracer in $Pd_{81}Si_{19}$ (#10), and Chen et al.[15] measured the diffusivity of Au in PdCuSi samples with different annealing treatments (#7-9). The extrapolation of Gupta et al.'s results seems to coincide with the measurements of Chen et al. on an as quenched sample (#8). Preannealing of a sample 10°K below T_g allows structural relaxation and leads to a decrease in diffusivity by almost two orders of magnitude (#7). This correlates with the viscosity increase observed in creep experiments after annealing (#5 and 6). One feature of these annealing experiments remains somewhat puzzling, however: one would expect that more structural relaxation would have occurred during the diffusion experiments in the 'as quenched' samples than during the preanneal, since the experiments were done at only slightly lower temperatures and for much longer times. It is surprising, therefore, that the diffusivity in the 'as quenched' samples remains high. The only possible explanation is that the rate of structural relaxation falls precipitously over a temperature interval of only a few degrees, while the diffusivity remains essentially unchanged. It is difficult to devise a structural argument that would reconcile these two phenomea, and additional investigation into this question seems to be required.

In spite of this problem, the diffusion results still provide some useful insights into the relation between the time constants τ_η, τ_D and τ_V. In configurational equilibrium, above T_g, (#9) the diffusivity scales with the shear viscosity, in accordance with the Stokes-Einstein relation which is known to hold at low viscosities ($\tau_D = \tau_\eta$). Below T_g, τ_D seems to be many orders of magnitude smaller than the extrapolation of τ_η from the creep experiments. However, if the activation energy for truly iso-configurational creep turns out to be larger than what has been measured up to now, the creep results could possibly be made to coincide with the diffusion results. The most important observation is concerned with the relation between the diffusion rate and the rate of structural relaxation. In order to observe measurable broadening of the concentration profile in a diffusion experiment, it is necessary to allow several hundred diffusive jumps per atom. If the time constants for structural relaxation and diffusion were the same ($\tau_V = \tau_D$), one jump per atom would suffice to reach the new equilibrium structure. However, since in all the experiments the observed diffusivity remains several orders of magnitude larger than the equilibrium diffusivity (i.e., in the fully relaxed configuration), the rate of structural relaxation must be much slower than the diffusion rate, or $\tau_V >> \tau_D$.

A possible explanation for this difference will be presented after a discussion of the defect model studies.

Finally, it is worthwhile to note that, as Chen et al. point out, the diffusivity of Au in amorphous PdCuSi is much smaller than the grain boundary diffusivity of Au in crystalline Pd, which argues against the presence of localized correlated defects such as grain boundaries or dislocation cores. For this reason the diffusivity in partially crystallized samples is also found to be higher than in fully amorphous ones.

c. Crystal growth

As has been pointed out in previous reviews,[17,18] the time constant for crystallization or phase separation above T_g scales as that for flow or diffusion. This is to be expected if the transformation involves redistribution of the chemical constituents by a diffusion mechanism $\tau_c = \tau_D$, and hence, above T_g, as discussed in the previous section, $\tau_c = \tau_D = \tau_\eta$.

If no such diffusive transport is necessary, for example in single phase crystallization without impurity redistribution, the time constant for crystallization can be much smaller than that for diffusion or flow $\tau_c \ll \tau_D, \tau_\eta$. The amount of structural relaxation attending crystallization below T_g is as yet unknown and more experiments are necessary to establish the relation between τ_c and τ_D below T_g.

III. MODEL STUDIES OF DEFECTS

1. Illustration by Means of a Two-Dimensional Model

a. Two-dimensional amorphous models

In two dimensions, it seems to be impossible to obtain a stable dense amorphous array of identical particles with an isotropic interaction potential. At least empirically, all observed dense arrays of identical hard spheres,[19] soap bubbles[20] or magnetic bubbles[21] are made up of hexagonal crystals. This is in contrast with the three-dimensional case, where a stable dense amorphous array of identical particles does exist, as exemplified by the dense random packing of hard spheres,[22] which is topologically distinct from the crystalline close packed arrays. Although no rigorous proof for this difference between two- and three-dimensional packing has been given, it can be made plausible as follows.

In three dimensions, the densest possible local configuration is a tetrahedral arrangement of four particles. Further local close packing of these tetrahedra leads to the formation of units with fivefold rotational symmetry. This in turn precludes translational symmetry and leads to the formation of an amorphous array. In other words: the basic feature of the dense random packing is its maximum short range density. The close packed crystalline structures are those of maximum long range density. The short range packing in these structures is quite distinct from that in the amorphous structure, since it requires the inclusion of a large number of octahedra.

In two dimensions, the densest possible local configuration is a triangle. Local close packing of these triangles, however, leads to the formation of hexagonal units, which is precisely what is needed to form a crystalline array. No distinct amorphous array can be formed. Or in summary: in two dimensions, the requirements for maximum short range and long range density coincide; in three dimensions they do not, and give rise to fundamentally distinct structures.

The only way, therefore, to obtain a two-dimensional amorphous array is to use a mixture of different particles, e.g., hard spheres of different sizes.[19] Figure 2a shows an example. Although these arrays are similar to the three-dimensional amorphous arrays, in the sense that they lack translational symmetry, they still retain some special properties on account of their two-dimensionality. This is illustrated on Fig. 2b, which shows the network formed by connecting the centers of the Dirichlet (or Wigner-Seitz) neighbors of Fig. 2a. It is easy to show that by this procedure the plane is completely and uniquely divided up in triangles, such that a circle through the vertices of a triangle contains no other sphere centers. For a very large network, Euler's relation between the number of vertices (V), edges (E), and faces (F) becomes $V - E + F = 0$. Since all the faces are triangles $F = 2E/3$, which leads to $E = 3V$. This means, as has been pointed out before,[23] that the average number of Dirichlet nearest neighbors is always six. This is obviously the case for each individual sphere in a crystalline array. Amorphous arrays contain spheres with different coordination numbers (5, 6 and 7 in Fig. 2a, e.g.); the average coordination number, however, must always be six. One might speculate that it is possible to characterize the structure of these two-dimensional amorphous arrays by the distribution of the coordination numbers around six.

b. Dynamic hard sphere experiments

In order to study the defects in these two-dimensional amorphous arrays a dynamic hard sphere simulator was used, similar to the one described by Turnbull and Cormia.[24] The apparatus consists of an horizontal 11'' diameter tray, with a flat glass plate at the bottom. The tray vibrates vertically with a frequency of 100 Hz. The amorphous array consisted of a mixture of an equal number of 3/16'' brass spheres and 5/32'' aluminum spheres. The total number of spheres was around 3000, which corresponds to a density of about 90% of the (phase separated) crystalline close packing. The dynamic properties of the system were analyzed by recording the motion on videotape. On replay, still photographs of the various instantaneous configurations of the system were obtained.

c. Analysis of the collapse of a 'vacancy'

A 'vacancy' in the amorphous array was created by picking out a sphere wile the system was in motion. This was done for both kinds of spheres and at a variety of (high) densities. In all these cases it was observed that the vacancy always collapsed. The free volume created was immediately redistributed and the vacancy lost its identity as a localized point defect. This is in sharp contrast with similar dynamic hard sphere observations of vacancies in crystalline arrays. Due to the lattice periodicity, the vacancies remain localized and even when they move, they retain their identity.

Figures 3 to 8 show a sequence of configurations illustrating this collapse. Also shown are the corresponding networks formed by connecting Dirichlet nearest neighbors. As shown on Fig. 3b, the creation of a vacancy results in an 8-fold coordination for one sphere, and a 5-fold coordination for two others to preserve the average. The same is true for a crystalline vacancy (see Fig. 9), and the presence of a high coordination number can be taken as characteristic for a localized vacancy. Indeed, as the subsequent configurations show, the disintegration of the vacancy corresponds to the disappearance of the 8-fold coordination.

It can also be observed that most configurational rearrangements involve spheres with a coordination number other than six. They can be considered as "special sites" that contribute to the redistribution of the vacancy volume. Furthermore, it can be seen that in the later stages of the collapse sequence the density of the array has increased, i.e., the vacancy has not only been redistributed, but has also, at least partially, been annihilated. This means that some of the "special sites" have long range elastic strain fields, such that upon rearrangement at that site, the displacements of the local collapse can be transferred to the specimen boundary.

2. Generalization to Three Dimensions

The previous demonstration-experiment was concerned with a point (i.e., zero-dimensional) defect in a two-dimensional amorphous array. Generalization of the conclusions for three-dimensional arrays and for other types of defects (one- and two-dimensional) is necessarily quite speculative since equivalent model experiments have not yet been done, but it is possible to make some reasonable predictions.

a. Point defects

Since it is the absence of lattice periodicity which allows the extra free volume of a vacancy to be redistributed, one would expect that an atomic-size vacancy in a three-dimensional random packing would also lose its identity by breaking up in small partial vacancies, which are in fact no more than small local perturbations of the SRO. Recent molecular dynamics studies seem to confirm this.[25] Furthermore, the idea of "special sites" with a long range elastic strain field where this extra free volume can be annihilated is also easily extended to three dimensions.

b. Line defects

As discussed above, the formation of localized shear bands during plastic deformation of amorphous metals at high stresses and low temperatures does not necessarily mean that they are formed by the equivalent of microscopically localized crystalline dislocations. In fact, because of configurational rearrangements made possible by the lack of translational symmetry it is likely that such a defect, when created 'artificially' in a model system, would also become diffuse and lose its identity. One can imagine creating such an 'artificial' microscopic dislocation in an amorphous model by the continuum procedure of making a planar cut through half the model and displacing the material on one side by a Burgers vector on the order of an atomic diameter. Provided the cut can then be rejoined (which is by no means certain, since translational symmetry, which assures perfect rejoining when creating a crystalline dislocation this way, is absent here) one obtains a dislocation which is localized at the end line of the planar cut. It is likely, however, that this configuration will change as soon as local rearrangements are allowed: small 'partial vacancies' can annihilate at the dislocation and make it climb, the line can react with the internal stress fields and be displaced, etc. Since all these rearrangements occur on an atomic scale, the initially straight dislocation line will become very contorted on the same scale. The concept of a localized core then loses its meaning. When a stress is applied, the local shear produced by one individual little segment of this contorted 'dislocation' is uncorrelated with that produced by the other segments. It is, therefore, more fruitful to think of the deformation process as being governed by the local shear of individual sites, rather than by the correlated motion of a crystalline-like dislocation line.

c. Planar defects

It is conceivable that the development of short range order in amorphous metals is a process which starts at various points in the specimen and grows as domains with a different spatial distribution of short range order (e.g., direction of tetrahedral stacking for topological SRO). Where two of these domains meet there must be a transition zone. In crystalline materials, again, the translational symmetry limits this zone to a sharp, well defined grain boundary plane.[26] In amorphous metals, this zone is likely to be more diffuse and can probably be described as a layer in which some of the atoms have imperfect SRO, different from that in either domain.

IV. CONCLUSIONS

From the above discussion it becomes clear that the most fruitful description of defects in amorphous metals is not in terms of localized point, line or planar defects as in crystals, but as local "special sites" where the SRO deviates from that in the "ideal glass" and therefore configurational rearrangements are possible. In the case of topological SRO, this deviation can be characterized by local presence of a certain small amount of 'free volume'. Turnbull and Cohen[27-29] have described the redistribution of this free volume and their treatment provides a way to estimate the number sites with a specific local free volume.

The type of rearrangement at these special sites, however, has heretofore never been clearly described. It has usually been assumed that all the defect sites were identical and were active in all atomic transport processes. It is suggested here that these special sites are not necessarily all identical, and that, depending on the details of the configuration, sites with different types of rearrangement can be distinguished.

For example, some of them can have a long range elastic strain field associated with them. They can annihilate free volume upon rearrangement and are therefore important for structural relaxation.

Another set can produce local shear and contributes to plastic flow. In homogeneous flow, the viscosity is determined by the concentration of these sites throughout the volume. If the process is truly iso-configurational, the steady-state concentration of shear sites is constant. The lifetime of each individual shear site is probably finite: upon shear rearrangement the free volume disappears locally, i.e., the SRO is restored and the site ceases to be a defect. The free volume, however, is not annihilated: it is redistributed and it combines with other 'fragments' to form new shear sites at other locations, resulting in a constant steady-state concentration. In inhomogeneous flow, a dynamic equilibrium is established between the creation of more shear sites due to stress-induced dilatation and the annihilation of these sites by structural relaxation. This leads to localization of the flow in a narrow band, where the shear site concentration is much higher and the viscosity much lower than in the bulk of the specimen.

A third set of sites are those which upon rearrangement lead to a change in the local nearest neighbor configuration and hence contribute to diffusion. Some of the shear and relaxation sites are probably also part of this third set: some of the shear and relaxation rearrangements no doubt lead to nearest neighbor switches. The rest of the set consists of sites which are loosely enough coupled to their surroundings that the only effect of rearrangement is a nearest neighbor change. In an iso-configurational diffusion process, again a steady-state concentration of diffusion sites is established as a result of local disappearance of free volume upon rearrangement of a site and its recombination and reappearance at a new diffusion site. If the process is not iso-configurational, i.e., if there is concurrent structural relaxation, free volume is also being annihilated. This requires that free volume is assembled at the 'relaxation sites' described in a previous paragraph. It is quite conceivable that the concentration of relaxation sites, which requires the presence of a long range elastic strain field, would be much smaller than the concentration of diffusion sites. This would be a possible explanation for the observed difference, below T_g, between the time constants for diffusion and structural relaxation ($\tau_D \ll \tau_V$).

In general, it can be concluded that the relation between the time constants for the various atomic transport processes must be determined by the relative concentrations and lifetimes of these various types of 'special sites'. A more detailed description of the possible rearrangements as a function of the changes in SRO is necessary, however, to make the approach quantitative and to allow detailed comparisons with experiment.

ACKNOWLEDGMENTS

I want to thank Professor D. Turnbull for many discussions which contributed considerably to the ideas developed in this paper, and for a critical review of the manuscript. The author's research in this field has been supported by the Office of Naval Research under Contract No. N00014-77-C-0002.

REFERENCES

1. D. Turnbull, Scripta Met., 11, 1131 (1977).

2. H. S. Chen and S. Y. Chuang, Phys. Stat. Sol. (a), 25, 581 (1974).

3. S. Y. Chuang, S. J. Tao and H. S. Chen, J. Phys. F. (Met. Phys.), 5, 1681 (1975).

4. M. Doyama, S. Tanigawa, K. Kuribayashi, H. Fukushima, K. Hinode and F. Saito, J. Phys. F (Met. Phys.) 5, L230 (1975).

5. H. S. Chen and S. Y. Chuang, J. Electr. Mater., 4, 783 (1975).

6. J. J. Gilman, J. Appl. Phys., 44, 675 (1973).

7. J. C. M. Li, in "Frontiers in Materials Science" (Ed. by L. E. Murr and C. Stein, Marcel Dekker, 1976), pp. 527-48.

8. D. E. Polk and D. Turnbull, Acta Met., 20, 493 (1972).

9. F. Spaepen, Acta Met., 25, 407 (1977).

10. A. S. Argon, to be published.

11. H. S. Chen and M. Goldstein, J. Appl. Phys., 43, 1642 (1971).

12. H. S. Chen and D. Turnbull, J. Chem. Phys., 48, 2560 (1968).

13. R. Maddin and T. Masumoto, Mat. Sci. Eng., 9, 153 (1972).

14. J. Logan and M. F. Ashby, Acta Met., 22, 1047 (1974).

15. H. S. Chen, L. C. Kimerling, J. M. Poate and W. L. Brown, Appl. Phys. Lett., 32, 461 (1978).

16. D. Gupta, K. N. Tu and K. W. Asai, Phys. Rev. Letters, 35, 796 (1975).

17. F. Spaepen and D. Turnbull, in "Metallic Glasses", A.S.M. Materials Science Seminar (Metals Park, Ohio, 1976), pp. 114-27.

18. D. Turnbull and B. G. Bagley, Treatise on Solid State Chemistry, 5 (ed. by N. B. Hannay, Plenum, N.Y., 1975), pp. 513-554.

19. A. S. Nowick and S. Mader, I.B.M. J. Res. and Dev., 9, 358 (1965).

20. W. L. Bragg and J. F. Nye, Proc. Roy. Soc., A190, 474 (1947).

21. P. Chaudhari, J. J. Cuomo and R. J. Gambino, I. B. M. J. Res. and Dev., 17, 66 (1973).

22. J. D. Bernal, Proc. Roy. Soc. (London), A280, 299 (1964).

23. J. L. Finney, Proc. Roy. Soc. (London), A319, 479 (1970).

24. D. Turnbull and R. L. Cormia, J. Appl. Phys., 31, 674 (1960).

25. P. Chaudhari, private communication (1977).

26. H. Gleiter and B. Chalmers, Progress in Materials Science (Ed. by B. Chalmers, J. W. Christian and T. B. Massalski, Pergamon, Oxford, 1972), pp. 1-4.

27. M. H. Cohen and D. Turnbull, J. Chem. Phys., 31, 1164 (1959).

28. D. Turnbull and M. H. Cohen, J. Chem. Phys., 34, 120 (1961).

29. D. Turnbull and M. H. Cohen, J. Chem. Phys., 52, 3038 (1970).

FIGURE CAPTIONS

Fig. 1: Flow and diffusion data for some amorphous metals. (Viscosity and diffusivity are scaled by the Stokes-Einstein relation.)

Flow data:

1) $Au_{77}Si_{14}Ge_9$ melt (8)
2) $Pd_{77.5}Cu_6Si_{16.5}$ equilibrium (11)
3) $Au_{77}Si_{14}Ge_9$ iso-configurational (12)
4) $Pd_{80}Si_{20}$ iso-configurational (?) (13)
5) $Co_{75}P_{25}$ iso-configurational (?) 1st run (14)
6) $Co_{75}P_{25}$ iso-configurational (?) rerun (14)

Diffusion data:

7) Au in $Pd_{77.5}Cu_6Si_{16.5}$ (annealed) (15)
8) Au in $Pd_{77.5}Cu_6Si_{16.5}$ ('as quenched') (15)
9) Au in $Pd_{77.5}Cu_6Si_{16.5}$ (equilibrium) (15)
10) Ag in $Pd_{81}Si_{19}$ (16)

Figs. 2-8: Sequence of configurations illustrating the collapse of a 'vacancy' created (at $t=1$, Fig. 3) in a two-dimensional amorphous dynamic hard sphere system. The number in the rectangular frame is the time (in arbitrary units).

(a) Actual configuration, showing the individual sphere positions in the vicinity of the vacancy. (The total number of spheres in the system is more than 3000.)

(b) Triangulated net, obtained by connecting the centers of the Dirichlet neighbors in the configuration of (a). Centers with 5, 7 or 8-fold coordination are marked.

Fig. 9: Triangular net formed by the Dirichlet neighbors associated with a vacancy in a two-dimensional crystalline (hexagonal) array, showing the characteristic 8-fold coordination. (This center has been moved infinitesimally towards the center of the vacancy in order to lift the degeneracy.)

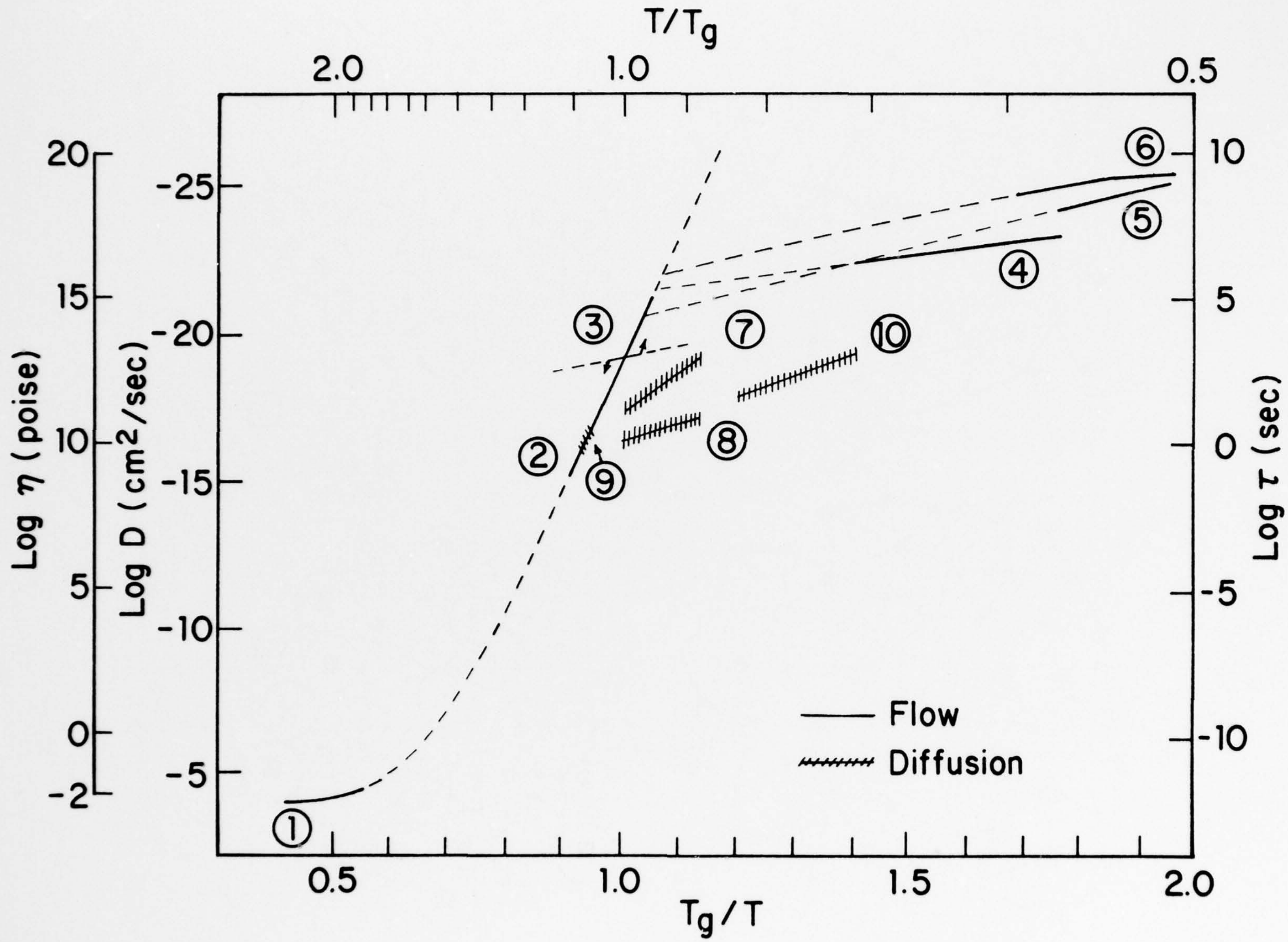
T/Tg
2.0
1.0
0.5
Log η (poise)
20
15
10
5
0
-2
Log D (cm2/sec)
-25
-20
-15
-10
-5
Log τ (sec)
10
5
0
-5
-10
1
2
3
4
5
6
7
8
9
10
Flow
Diffusion
0.5
1.0
1.5
2.0
Tg/T

Figure 1

0

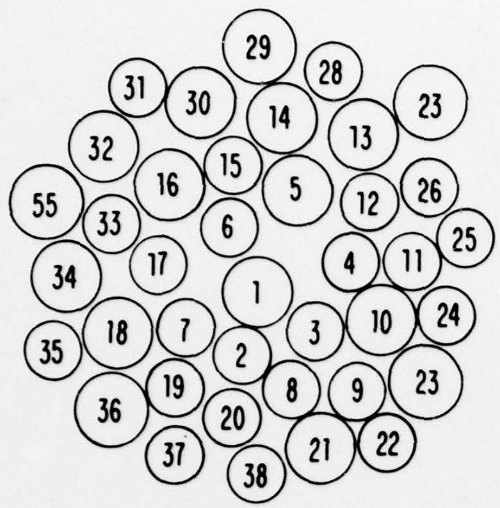

Figure 2a

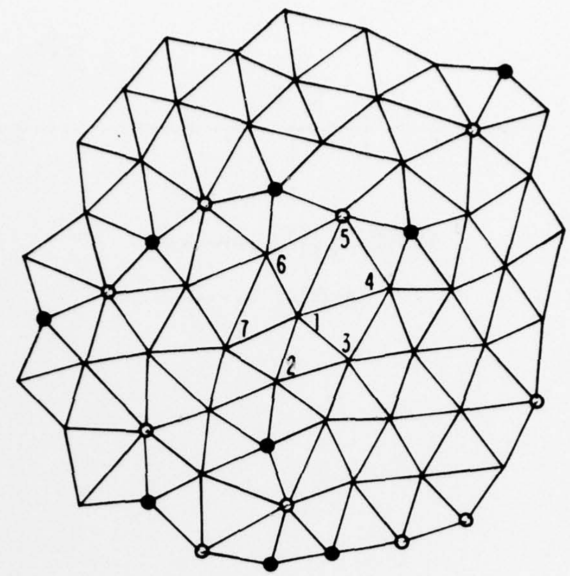

Figure 2b

1

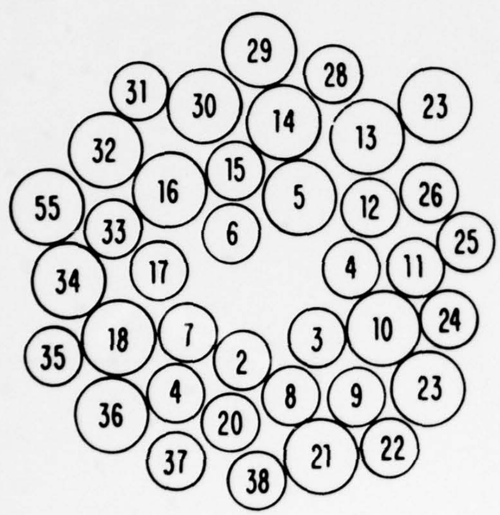

Figure 3a

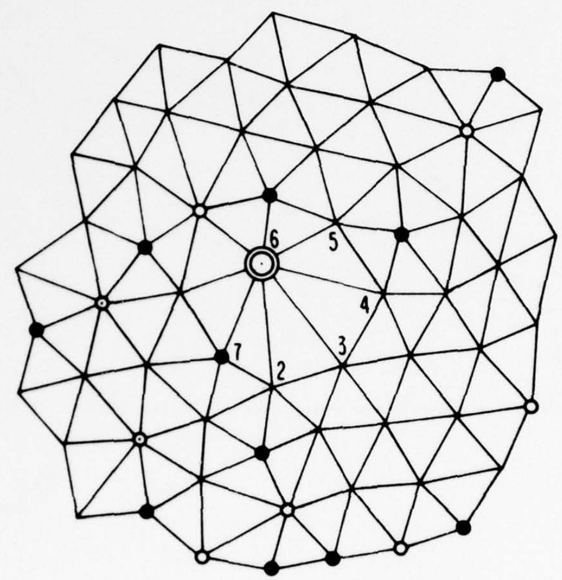

Figure 3b

2

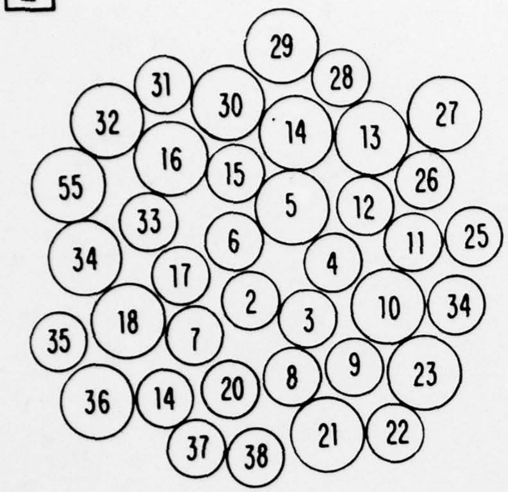

Figure 4a

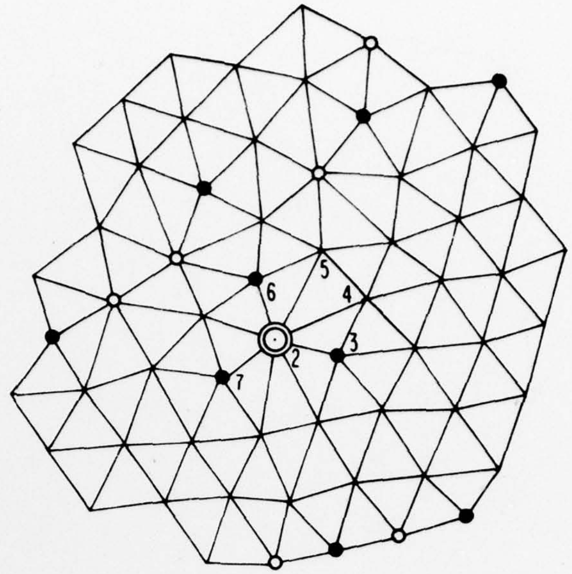

Figure 4b

6

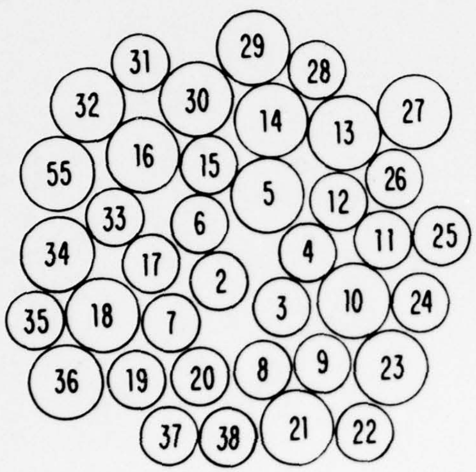

Figure 5a

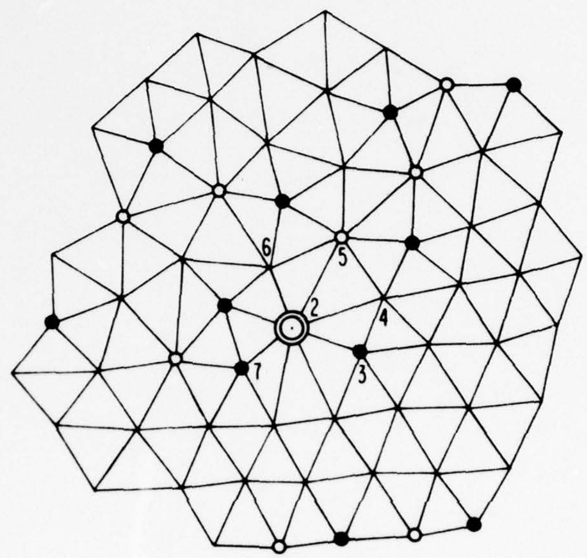

Figure 5b

7

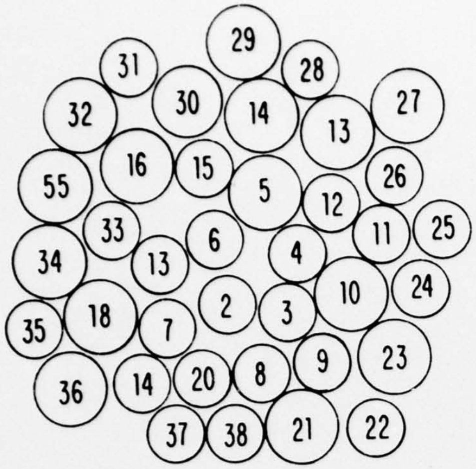

Figure 6a

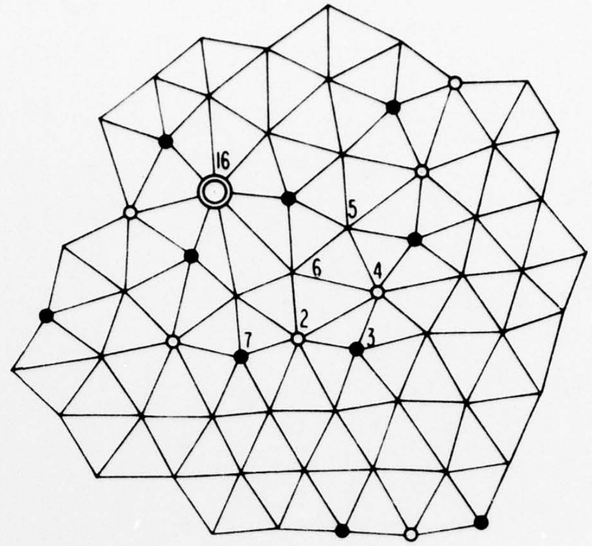

Figure 6b

13

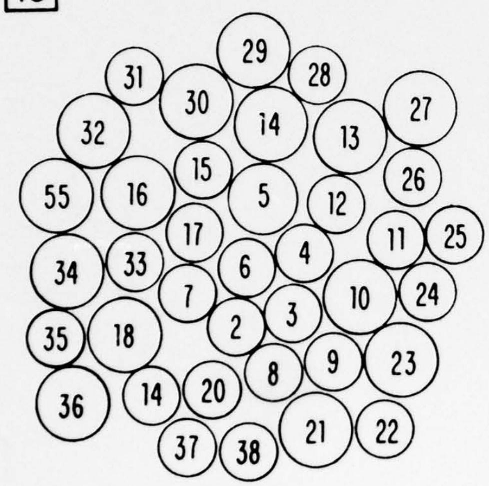

Figure 7a

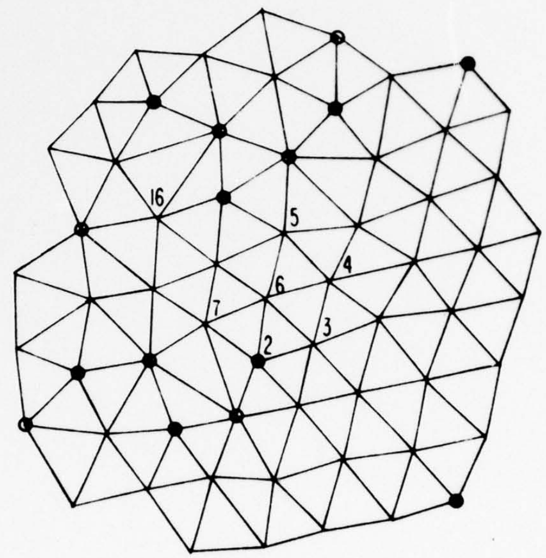

Figure 7b

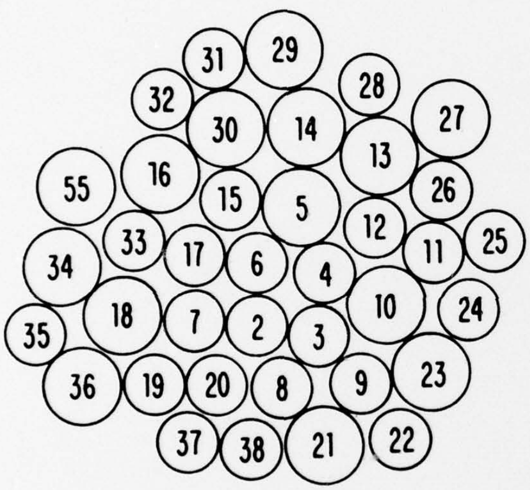
31
29
32
28
30
14
27
13
55
16
15
5
26
12
25
33
17
6
11
34
4
10
24
18
7
2
3
35
23
36
19
20
8
9
37
38
21
22

(a)

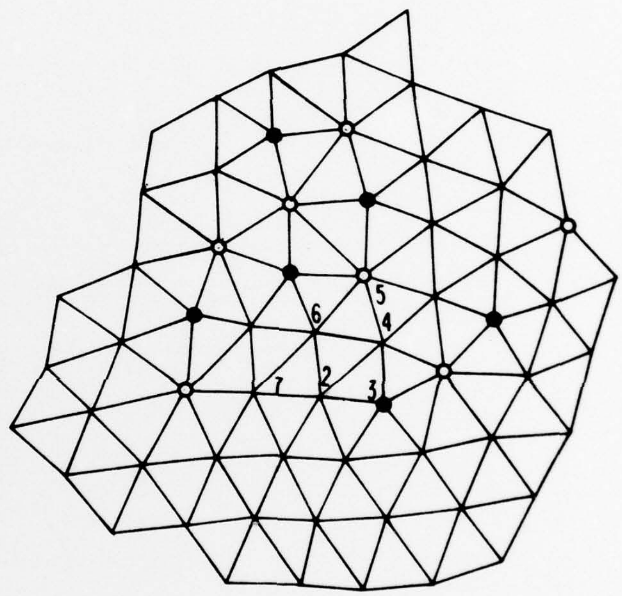
5
6
4
7
2
3

(b)

Figure 8

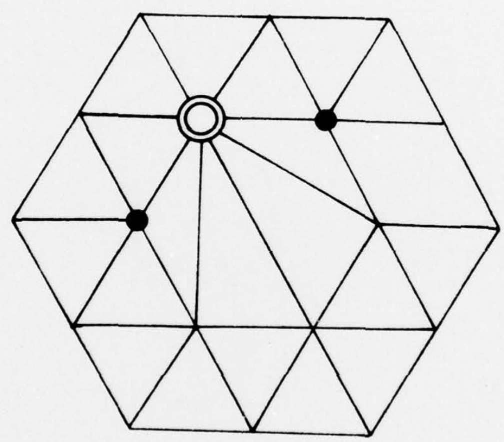

Figure 9

Defense Documentation Center
Cameron Station
Alexandria, Virginia 22314 (12)

Office of Naval Research
Department of the Navy

Attn: Code 471 (3)
Code 105 (6)
Code 470

Director
Office of Naval Research
Branch Office
495 Summer Street
Boston, Massachusetts 02210

Director
Office of Naval Research
Branch Office
536 South Clark Street
Chicago, Illinois 60605

Office of Naval Research
San Francisco Area Office
760 Market Street, Room 447
San Francisco, California 94102

Naval Research Laboratory
Washington, D.C. 20390

Attn: Code 6000
Code 6100
Code 6300
Code 6400
Code 2627 (6)

Attn: Mr. F.S. Williams
Naval Air Development Center
Code 302
Warminster, Pennsylvania 18974

Naval Air Propulsion Test Center
Trenton, New Jersey 08628
Attn: Library

Naval Weapons Laboratory
Dahlgren, Virginia 22448
Attn: Research Division

Naval Construction Batallion
Civil Engineering Laboratory
Port Hueneme, California 93043
Attn: Materials Division

Naval Electronics Laboratory Center
San Diego, California 92152
Attn: Electronic Materials Sciences Div.

Naval Missile Center
Materials Consultant
Code 3312-1
Point Mugu, California 93041

Commanding Officer
Naval Ordnance Laboratory
White Oak
Silver Spring, Maryland 20910
Attn: Library

Naval Ship R. and D. Center
Materials Department
Annapolis, Maryland 21402

Naval Undersea Center
San Diego, California 92132
Attn: Library

Naval Underwater System Center
Newport, Rhode Island 02840
Attn: Library

Naval Weapons Center
China Lake, California 93555
Attn: Library

Naval Postgraduate School
Monterey, California 93940
Attn: Materials Sciences Dept.

Naval Air Systems Command
Washington, D.C. 20360

Attn: Code 52031
Code 52032
Code 320

Naval Sea System Command
Washington, D.C. 20362
Attn: Code 035

Naval Facilities
Engineering Command
Alexandria, Virginia 22331
Attn: Code 03

Scientific Advisor
Commandant of the Marine Corps
Washington, D.C. 20380
Attn: Code AX

Naval Ship Engineering Center
Department of the Navy
Washington, D.C. 20360
Attn: Director, Materials Sciences

Army Research Office
Box CM, Duke Station
Durham, North Carolina 27706
Attn: Metallurgy and Ceramics Div.

Army Materials and Mechanics
Research Center
Watertown, Massachusetts 02172
Attn: Res. Programs Office (AMXMR-P)

Commanding General
Department of the Army
Frankford Arsenal
Philadelphia, Pennsylvania 19137
Attn: ORDBA-1320

Office of Scientific Research
Department of the Air Force
Washington, D.C. 20333
Attn: Solid State Div. (SRPS)

Aerospace Research Labs
Wright-Patterson AFB
Building 450
Dayton, Ohio 45433

Air Force Materials Lab (LA)
Wright-Patterson AFB
Dayton, Ohio 45433

NASA Headquarters
Washington, D.C. 20546
Attn: Code RRM

NASA
Lewis Research Center
21000 Brookpark Road
Cleveland, Ohio 44135
Attn: Library

National Bureau of Standards
Washington, D.C. 20234

Attn: Metallurgy Division
Inorganic Materials Division

Atomic Energy Commission
Washington, D.C. 20545
Attn: Metals and Materials Branch

Defense Metals and Ceramics
Information Center
Battelle Memorial Institute
505 King Avenue
Columbus, Ohio 43201

Director
Ordnance Research Laboratory
P.O. Box 30
State College, Pennsylvania 16801

Director Applied Physics Lab.
University of Washington
1013 Northeast Fortieth Street
Seattle, Washington 98105

Metals and Ceramics Division
Oak Ridge National Laboratory
P.O. Box X
Oak Ridge, Tennessee 37830

Los Alamos Scientific Lab.
P.O. Box 1663
Los Alamos, New Mexico 87544
Attn: Report Librarian

Argonne National Laboratory
Metallurgy Division
P.O. Box 229
Lemont, Illinois 60439

Brookhaven National Laboratory
Technical Information Division
Upton, Long Island
New York 11973
Attn: Research Library

Library
Building 50, Room 134
Lawrence Radiation Laboratory
Berkeley, California

Professor G.S. Ansell
Rensselaer Polytechnic Institute
Dept. of Metallurgical Engineering
Troy, New York 12181

Professor H.K. Birnbaum
University of Illinois
Department of Metallurty
Urbana, Illinois 61801

Dr. E.M. Breinan
United Aircraft Corporation
United Aircraft Research Lab.
East Hartford, Connecticut 06108

Professor H.D. Brody
University of Pittsburgh
School of Engineering
Pittsburgh, Pennsylvania 15213

Professor J.B. Cohen
Northwestern University
Dept. of Material Sciences
Evanston, Illinois 60201

Professor M. Cohen
Massachusetts Institute of Technology
Department of Metallurgy
Cambridge, Massachusetts 02139

Professor B.C. Giessen
Northeastern University
Department of Chemistry
Boston, Massachusetts 02115

Dr. G.T. Hahn
Battelle Memorial Institute
Department of Metallurgy
505 King Avenue
Columbus, Ohio 43201

Professor R.W. Heckel
Carnegie-Mellon University
Schenley Part
Pittsburgh, Pennsylvania 15213

Dr. David G. Howden
Battelle Memorial Institute
Columbus Laboratories
505 King Avenue
Columbus, Ohio 43201

Professor C.E. Jackson
Ohio State University
Dept. of Welding Engineering
190 West 19th Avenue
Columbus, Ohio 43210

Professor G. Judd
Rensselaer Polytechnic Institute
Dept. of Materials Engineering
Troy, New York 12181

Dr. C.S. Kortovich
TRW, Inc.
23555 Euclid Avenue
Cleveland, Ohio 44117

Professor D.A. Koss
Michigan Technological University
College of Engineering
Houghton, Michigan 49931

Professor A. Lawley
Drexel University
Dept. of Metallurgical Engineering
Philadelphia, Pennsylvania 19104

Dr. H. Margolin
Polytechnic Institute of New York
333 Jay Street
Brooklyn, New York 11201

Professor K. Masabuchi
Massachusetts Institute of Technology
Department of Ocean Engineering
Cambridge, Massachusetts 02139

Dr. G.H. Meier
University of Pittsburgh
Dept. of Metallurgical and Materials
Engineering
Pittsburgh, Pennsylvania 15213

Professor J.W. Morris, Jr.
University of California
College of Engineering
Berkeley, California 94720

Professor K. Ono
University of California
Materials Department
Los Angeles, California 90024

Professor W.F. Savage
Rensselaer Polytechnic Institute
School of Engineering
Troy, New York 12181

Dr. C. Shaw
Rockwell International Corp.
P.O. Box 1085
1049 Camino Dos Rios
Thousand Oaks, California 91360

Professor O.D. Sherby
Stanford University
Materials Sciences Dept.
Stanford, California 94300

Professor J. Shyne
Stanford University
Materials Sciences Department
Stanford, California 94300

Dr. W.A. Spitzig
U.S. Steel Corporation
Research Laboratory
Monroeville, Pennsylvania 15146

Dr. E.A. Starke, Jr.
Georgia Institute of Technology
School of Chemical Engineering
Atlanta, Georgia 30332

Professor N.S. Stoloff
Rensselaer Polytechnic Institute
School of Engineering
Troy, New York 12181

Dr. E.R. Thompson
United Aircraft Research Lab.
400 Main Street
East Hartford, Connecticut 06108

Professor David Turnbull
Harvard University
Division of Engineering and Applied
Physics
Cambridge, Massachusetts 02139

Dr. F.W. Wang
Naval Ordnance Laboratory
Physics Laboratory
White Oak
Silver Spring, Maryland 20910

Dr. J.C. Williams
Rockwell International
Science Center
P.O. Box 1085
Thousand Oaks, California 91360

Professor H.G.F. Wilsdorf
University of Virginia
Department of Materials Science
Charlottesville, Virginia 22903

Dr. M.A. Wright
University of Tennessee
Space Institute
Dept. of Metallurgical Engineering
Tullahoma, Tennessee 37388